Developmental Science

Developmental Science 19:4 (2016), pp 686–695 DOI: 10.1111/desc.12443

SPECIAL ISSUE ARTICLE

Altered functional connectivity of the default mode network in Williams syndrome: a multimodal approach

Adriana Sampaio,[1] Pedro Silva Moreira,[2,3] Ana Osório,[1,4] Ricardo Magalhães,[2,3] Cristiana Vasconcelos,[6] Montse Férnandez,[5] Angel Carracedo,[5] Joana Alegria,[1] Óscar F. Gonçalves[1,7,8] and José Miguel Soares[2,3]

1. *Neuropsychophysiology Lab, CIPsi, School of Psychology, University of Minho, Portugal*
2. *Life and Health Sciences Research Institute (ICVS), School of Health Sciences, University of Minho, Portugal*
3. *ICVS/3B's – PT Government Associate Laboratory, Braga/Guimarães, Portugal*
4. *Social and Cognitive Neuroscience Lab, Post-Graduate Program on Developmental Disorders – Center for Biological and Health Sciences, Mackenzie Presbyterian University, São Paulo, Brazil*
5. *Genetic Molecular Unit, Galician Public Foundation of Genomic Medicine, University of Santiago de Compostela, Spain*
6. *Department of Neuroradiology, CHP - Hospital Santo António, Porto, Portugal*
7. *Spaulding Neuromodulation Center, Department of Physical Medicine & Rehabilitation, Spaulding Rehabilitation Hospital and Massachusetts General Hospital, USA*
8. *Department of Applied Psychology, Bouvé College of Health Sciences, Northeastern University, USA*

Abstract

*Resting state brain networks are implicated in a variety of relevant brain functions. Importantly, abnormal patterns of functional connectivity (FC) have been reported in several neurodevelopmental disorders. In particular, the Default Mode Network (DMN) has been found to be associated with social cognition. We hypothesize that the DMN may be altered in Williams syndrome (WS), a neurodevelopmental genetic disorder characterized by an unique cognitive and behavioral phenotype. In this study, we assessed the architecture of the DMN using fMRI in WS patients and typically developing matched controls (sex and age) in terms of FC and volumetry of the DMN. Moreover, we complemented the analysis with a functional connectome approach. After excluding participants due to movement artifacts (*n = *3), seven participants with WS and their respective matched controls were included in the analyses. A decreased FC between the DMN regions was observed in the WS group when compared with the typically developing group. Specifically, we found a decreased FC in a posterior hub of the DMN including the precuneus, calcarine and the posterior cingulate of the left hemisphere. The functional connectome approach showed a focalized and global increased FC connectome in the WS group. The reduced FC of the posterior hub of the DMN in the WS group is consistent with immaturity of the brain FC patterns and may be associated with the singularity of their visual spatial phenotype.*

Research highlights

- Abnormal patterns of the resting state functional connectivity (FC) have been reported in several neurodevelopmental disorders.
- Here, we assessed the architecture and volumetry of the Default Mode Network in Williams syndrome (WS) and in typically developing (TD) matched controls. A whole brain functional network (i.e. the functional connectome) approach was also employed.
- A decreased FC between the DMN regions and a global and inter-hemispheric FC connectome increase was observed in the WS group.
- The reduced FC of the posterior hub of the DMN in WS group is consistent with immaturity of the brain FC patterns and may be associated with the singularity of their visual spatial phenotype.

Address for correspondence: Adriana Sampaio, School of Psychology, University of Minho, 4710-057 Braga, Portugal; e-mail: adriana.sampaio@psi.uminho.pt

Introduction

Human brain function during resting state has become an important focus of interest in the search for the neural correlates of various neurodevelopmental disorders (Kennedy & Courchesne, 2008a, 2008b; Menon, Leroux, White & Reiss, 2004; Vega, Hohman, Pryweller, Dykens & Thornton-Wells, 2015). The default mode network (DMN) is one of the core resting state networks and is characterized by a pattern of activation and functional connectivity (FC) of several brain regions such as the medial prefrontal cortex (MPFC), the posterior cingulate cortex (PCC), precuneus (PrC) and bilateral inferior parietal cortex (IPC) (Raichle, MacLeod, Snyder, Powers, Gusnard *et al*., 2001). The DMN is thought to subserve internal mental activity detached from the external world, such as personal introspection, autobiographical memories and thoughts of the future, as well as connecting internal and external attention while monitoring the world around us (Buckner, Andrews-Hanna & Schacter, 2008; Greicius, Krasnow, Reiss & Menon, 2003; Mason, Norton, Van Horn, Wegner, Grafton *et al*., 2007). Although the DMN typically refers to a constellation of brain regions functionally more connected during 'rest', its regional deactivations also take place when we engage in attention demanding or goal-directed tasks. Therefore the DMN is also considered to be task negative (Broyd, Demanuele, Debener, Helps, James *et al*., 2009) as greater suppression of this network has been associated with better performance in several cognitive tasks (Mayer, Roebroeck, Maurer & Linden, 2010; Singh & Fawcett, 2008). Failure to deactivate and abnormal FC patterns of the DMN have been associated with several neuropsychiatric (Guerrero-Pedraza, McKenna, Gomar, Sarro, Salvador *et al*., 2012; Pomarol-Clotet, Salvador, Sarro, Gomar, Vila *et al*., 2008) and neurodevelopmental disorders (Kennedy & Courchesne, 2008a, 2008b; Menon *et al*., 2004; Vega *et al*., 2015). Moreover, most of the brain regions of the DMN have been found to overlap with important areas subserving social cognition. Meta-analyses of functional magnetic resonance imaging (fMRI) studies showed that specific brain networks involved in social-cognitive tasks match the different nodes of the DMN (Mars, Neubert, Noonan, Sallet, Toni *et al*., 2012). Particularly important are studies reporting an association between abnormalities in the FC of the DMN and poor social cognition (Holt, Cassidy, Andrews-Hanna, Lee, Coombs *et al*., 2011; Jung, Kosaka, Saito, Ishitobi, Morita *et al*., 2014; Kennedy & Courchesne, 2008a; von dem Hagen, Stoyanova, Baron-Cohen & Calder, 2013; Weng, Wiggins, Peltier, Carrasco, Risi *et al*., 2010).

In fact, the different DMN nodes play an important role in social stimuli processing, an ability found to be altered in Williams syndrome (WS), a neurodevelopmental disorder caused by a microdeletion in the long-arm of chromosome 7 (Korenberg, Chen, Hirota, Lai, Bellugi *et al*., 2000). Patients with WS display an unusual cognitive phenotype, characterized by intellectual disabilities with a distinctive neuropsychological profile with severe impairments in visuospatial cognition coexisting with a relative preservation of face recognition and narrative skills (Sampaio, Fernandez, Henriques, Carracedo, Sousa *et al*., 2009; Sampaio, Sousa, Fernandez, Henriques & Goncalves, 2008). In addition, individuals with WS show exacerbated interest in social stimuli and social interactions from an early age and across development, in clear contrast with other developmental disorders (Capitao, Sampaio, Fernandez, Sousa, Pinheiro *et al*., 2011a; Dykens & Rosner, 1999; Jones, Bellugi, Lai, Chiles, Reilly *et al*., 2000). Despite their gregarious personality, people with WS show marked difficulties in navigating within the social world. Data from parental report as well as direct observations suggest deficits in regulating and understanding social interactions which are often stronger than would be expected based on intellectual disability (Dodd, Porter, Peters & Rapee, 2010; Klein-Tasman, Li-Barber & Magargee, 2011; Laing, Butterworth, Ansari, Gsödl, Longhi *et al*., 2002). More recent evidence suggests that deficits in social cognition are associated with abnormal social reciprocity behaviors in WS (Van der Fluit, Gaffrey & Klein-Tasman, 2012).

Various lines of evidence support the hypothesis of abnormal DMN functioning in WS. Firstly, several nodes of the DMN have been reported to be abnormal in WS. For instance, structural neuroimaging studies have found alterations in the MPFC, including disproportionate enlargement as well as increased gyrification in WS, when compared with typically developing individuals (Capitao, Sampaio, Sampaio, Vasconcelos, Fernandez *et al*., 2011b; Gaser, Luders, Thompson, Lee, Dutton *et al*., 2006; Reiss, Eckert, Rose, Karchemskiy, Kesler *et al*., 2004). In addition, studies have found altered patterns of cortical folding in the PCC and left PrC in WS (Gaser *et al*., 2006). Post-mortem and MRI studies have also reported parietal hypoplasia as well as increased parietal grey matter volumes in WS, respectively (Galaburda & Bellugi, 2000; Reiss, Eliez, Schmitt, Straus, Lai *et al*., 2000). Secondly, it has previously been suggested that the relative overlap between the DMN and areas devoted to social cognition in typical development may reflect a general human readiness for social interaction (Mars *et al*., 2012; Mitchell, 2008). This is

corroborated by studies showing an association between lower FC and autism spectrum traits such as social deficits (Jung *et al.*, 2014; Kennedy & Courchesne, 2008a; von dem Hagen *et al.*, 2013; Weng *et al.*, 2010). Finally, a recent study examining the resting state FC in Down syndrome, WS and typically developing individuals showed that WS present increased between-network connectivity (e.g. frontoparietal-DMN network pair) and decreased within-network connectivity (e.g. DMN, ventral attention and somatomotor networks), when compared with typically developing individuals, suggesting a global lack of differentiation between the DMN and other resting state networks in WS (Vega *et al.*, 2015). These results may be related with specificities of the brain tissue organization in WS. Accordingly, abnormal patterns of cortical folding in the default mode regions reported in WS, which are conceivably linked with relative preservations of gray matter in the presence of reduced white matter, can also be considered an indicator of compromised white matter integrity within the DMN. Indeed, mounting evidence points to altered patterns of cortical-subcortical connectivity in this syndrome (e.g. Marenco, Siuta, Kippenhan, Grodofsky, Chang *et al.*, 2007). For instance, abnormal connections between the prefrontal cortex and the amygdala are believed to contribute to the WS social phenotype (Meyer-Lindenberg, Hariri, Munoz, Mervis, Mattay *et al.*, 2005; Meyer-Lindenberg, Kohn, Mervis, Kippenhan, Olsen *et al.*, 2004), and abnormal frontostriatal circuitry in conjunction with altered connectivity between the amygdala and the prefrontal cortex have been documented in many studies of WS (Gaser *et al.*, 2006; Gothelf, Searcy, Reilly, Lai, Lanre-Amos *et al.*, 2008; Meyer-Lindenberg *et al.*, 2004; Munoz, Meyer-Lindenberg, Hariri, Mervis, Mattay *et al.*, 2010).

Therefore, there is compelling evidence suggesting that WS may present altered patterns of whole brain FC and more specifically among the DMN regions, both functionally and structurally. In this study we used a functional connectome MRI approach to assess brain connectivity in WS in comparison with a typically developing group, studying the FC and volumetry of the DMN and the topological organization of the global functional connectomes.

Materials and methods

Participants

Ten participants (four males), diagnosed with WS (age 21.33 ± 6.75) were compared to 11 typically developing individuals (TD) (six males, age 22.00 ± 6.65). No significant age differences were evident between the two groups ($p > .05$). After excluding three participants with WS due to movement artifacts, seven participants with WS and only their respective matched (sex and age) control counterparts were included in the analyses (WS; three males and four females, mean age 23.00; $SD = 7.00$; TD, three males and four females, mean age 24.14, $SD = 6.12$).

Participants in the WS group tested positive in fluorescence in situ hybridization (FISH) for deletion of the elastin gene on chromosome 7. The presence of any sensorial or speech disorders, as well as comorbidity with severe psychopathology not associated with the syndrome, were defined as exclusion criteria. In the WS group, the Wechsler Intelligence Scale – WISC-III (Wechsler, 1991) and WAIS-III (Wechsler, 1997) were used to assess general cognitive functioning and the Block Design subtest, a measure of visuospatial functioning, in order to be used for correlational analysis with the FC of the DMN. The control group included typically developing individuals without a history of sensorial, psychiatric, neurological disorder or cognitive impairment, questions included in the socio-demographic questionnaire. The study was conducted in accordance with the principles expressed in the Declaration of Helsinki and was approved by the local ethics committee. The study goals and tests were explained to the participants or their legal guardians and all gave informed written consent.

Data acquisition

Participants were scanned on a clinically approved 3T Philips (Philips Achieva, Best, Netherlands) MRI scanner at a local hospital (CHP-HSA). The imaging sessions included one structural T1-weighted and one functional T2*-weighted acquisition conducted in the same day. For structural analysis, a T1 high-resolution anatomical sequence, 3D SENSitivity Encoding (SENSE) was performed with the following scan parameters: repetition time (TR) = 7.85 s, echo time (TE) = 4.00 ms, 170 sagittal slices with no gap, flip angle (FA) = 8°, in-plane resolution = 1.0 × 1.0 mm^2 and slice thickness = 2.0 mm. During the resting state fMRI scan (5 minutes of acquisition), using gradient echo weighted echo-planar images (EPIs), participants were instructed to keep their eyes closed and to think about nothing in particular. The imaging parameters were: 100 volumes, TR = 3 s, TE = 40 ms, FA = 90°, in-plane resolution = 3.0 × 3.0 mm^2, 45 interleaved slices, slice thickness = 3.2 mm, imaging matrix 72 × 74 and FoV = 235 mm.

Image pre-processing

Before any data processing and analysis, all acquisitions were visually inspected by a certified neuroradiologist who confirmed that they were not affected by critical head motion and that participants had no brain lesions. To achieve signal stabilization and allow participants to adjust to the scanner noise, the first three-fMRI volumes (9 seconds) were discarded. Resting state data preprocessing was performed using FMRIB Software Library (FSL v5.0.4, www.fmrib.ox.ac.uk/fsl). Images were first corrected for slice timing using the first slice as reference and Fourier phase shift interpolation. To correct for head motion, images were realigned to the mean image with a six-parameter rigid-body spatial transformation and estimation was performed at 0.9 quality, 4 mm separation, 5 mm full-width at half-maximum (FWHM) smoothing kernel and using 2nd degree B-Spline interpolation. Also, in order to reduce the potential contamination of motion on functional connectivity, motion scrubbing (Power, Barnes, Snyder, Schlaggar & Peterson, 2012) was performed. With this strategy, it was possible to identify and further exclude time-points where head motion could be critical. From this analysis, three WS and two TD participants were excluded (final sample in the analysis included a group of WS; $N = 7$, matched in gender and age with a TD group; $N = 7$). Images were then spatially normalized with a non-linear transformation to the MNI (Montreal Neurological Institute) standard coordinate system using the FSL template through the combination of the rigid-body co-registration matrix and warp of the nonlinear transformation. Data were then re-sampled to $3 \times 3 \times 3\ mm^3$ using sinc interpolation, smoothed to decrease spatial noise with an 8 mm FWHM, Gaussian kernel. Images were then temporally band-pass filtered (0.01–0.08 Hz) and grand mean-scaled. Finally, a linear regression of the motion parameters, mean white-matter (WM) and cerebrospinal (CSF) signals, and motion outliers was conducted.

For the graph analysis the pre-processing strategy was as described elsewhere (Magalhaes, Marques, Soares, Alves & Sousa, 2015). Briefly, the steps of slice timing correction, head motion correction, and band-pass filtering were used as described in the present work. To remove White Matter and Cerebrospinal Fluid confound signal an a-compcor strategy was employed (Behzadi, Restom, Liau & Liu, 2007), and the corresponding time series obtained. These were included in a general linear model with the movement regressors, the motion outliers from the scrubbing correction and the mean global signal, and the resulting residuals obtained were used as the data of interest. No smoothing or normalization was applied.

Structural analysis

The structural analysis based on segmentation of brain cortical and subcortical structures from T1 high-resolution anatomical data was performed using the Freesurfer toolkit version 5.1 (http://surfer.nmr.mgh.harvard.edu). Intracranial volume (ICV) was used to correct the regional volumes and the processing pipeline was the same as previously described (Soares, Sampaio, Ferreira, Santos, Marques *et al*., 2012). The DMN was defined by the summed volume of the angular gyrus of the inferior parietal lobe, the posterior cingulate, the precuneus and the frontopolar regions (Buckner *et al*., 2008; Raichle *et al*., 2001)

Functional connectivity analysis

Functional connectivity analysis was performed using a seed-driven approach with FSL. The seed ROI was defined as a 6 mm radius sphere centered on the PCC (1, −55, 17 MNI coordinates) following a previous study (Woodward, Rogers & Heckers, 2011). Dual-regression analysis was conducted to estimate the subject-specific component of the DMN.

Functional connectome construction and analysis

Connectome nodes were defined as the segmented regions from the Freesurfer workflow from 14 subcortical regions from the atlas (Fischl, Salat, Busa, Albert, Dieterich *et al*., 2002) and 68 cortical regions from the Desikan and collaborators atlas were used (Desikan, Segonne, Fischl, Quinn, Dickerson *et al*., 2006). The registration from anatomical to functional space, calculated in a previous step, was used to register the segmentation to functional space. Using these as masks, the mean time series over each region for each subject was extracted. Using the nitime library (Millman & Brett, 2007), the correlations between each subject time series were calculated using the Pearson correlation and the adjacency matrices thus obtained were converted to *z*-values using the Fisher transformation. Statistical testing on the adjacency matrices was carried out using Network Based Statistics (Zalesky, Fornito & Bullmore, 2010). Briefly, a two-sample *t*-test was applied to each connection in the connectome, which were then thresholded by a user-defined significance. To allow the identification of connectomes at different significances and extents, different thresholds at the connection level of $p = .01$, $p = .005$ and $p = .001$ were tested, as suggested by the authors of the Toolbox. The surviving connections were used to identify connectome components (groups of two or more regions connected by

significantly affected connections, in such a way that a path can be found between each pair of regions of the component), and its extents (number of connections in the component) were obtained. To test the component significance, a non-parametric test was used to test the significance of its extent: 5000 random permutations of the groups were generated and tested, allowing the identification of significant components at a significance level of $p = .05$.

Statistical analyses

For structural analysis (IBM SPSS Statistics software, v.22, IBM, New York), an Analysis of Covariance (ANCOVA) was performed to test for group differences in DMN volume, controlling for the total intracranial volume (ICV). DMN volumetric analysis was considered significant at $p < .05$. For functional analysis (SPM8 software), two-tailed independent-sample *t*-test was performed. One-sample *t*-test analyses were initially performed to confirm that DMN was obtained using the pre-defined ROI (see Figure 1) and further, a two-sample *t*-test between WS and Control group was conducted. Finally, for the WS group, a correlation analysis between the DMN FC and Block Design subtest performance was performed. Results were considered significant at $p < .05$ corrected for multiple comparisons using a combination of a peak threshold of $p < .005$ with a minimum cluster size (196 voxels). The minimum cluster size was determined over 1000 Monte Carlo simulations using the AlphaSim program distributed with the REST software tool (http://resting-fmri.sourceforge.net/) with the following input parameters: individual voxel probability threshold = 0.005, cluster connection radius = 2 mm, Gaussian filter width (FWHM) = 10 × 10 × 9 mm (smoothness estimated with 3dFWHMx program), number of Monte Carlo simulations = 1000 and mask was set to the DMN template mask. Anatomical labeling was defined by a combination of visual inspection and Anatomical Automatic Labeling Atlas (AAL) (Tzourio-Mazoyer, Landeau, Papathanassiou, Crivello, Etard *et al.*, 2002).

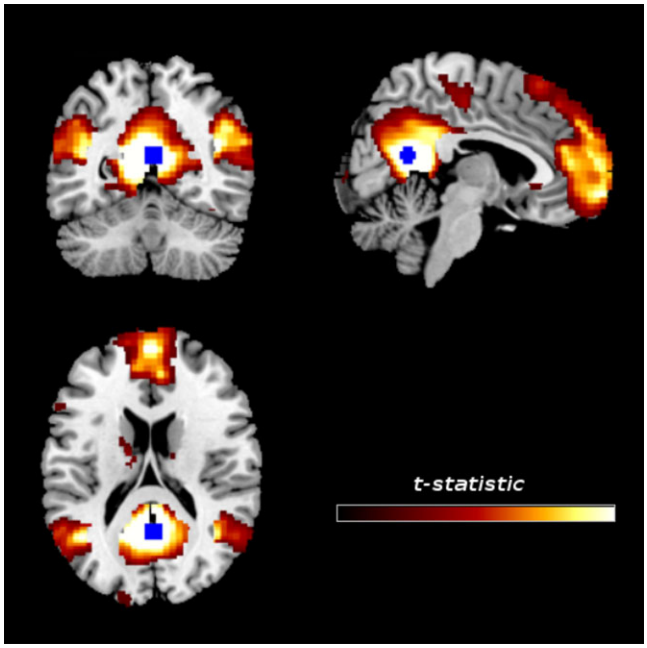

Figure 1 *One sample* t-*test results for the DMN in both groups (WS and TD), using the predefined ROI seed analysis (blue mark, 6 mm radius sphere centered on the PCC (1, −55, 17 MNI coordinates).*

Results

DMN volumetry

When controlling for ICV [$F_{(1,13)} = 4.27$, $p = .063$], participants with WS presented a trend to show increased volumes of the areas comprising the DMN ($M = 4.79\text{x}10^4$, $SE = 1721.19$) when compared to the TD group ($M = 4.23\text{x}10^4$, $SE = 1721.19$). In order to explore this trend, the volume of the individual regions comprising the DMN was compared between the groups. We observed that WS participants presented increased volumes of the left posterior cingulate [$F_{(1,13)} = 4.91$, $p = .049$], left frontal pole [$F_{(1,13)} = 8.25$, $p = .015$] and left postcentral gyrus [$F_{(1,13)} = 8.33$, $p = .015$]. The statistical significance of these differences was lost after correcting for multiple comparisons (Bonferroni correction).

DMN functional connectivity

Both groups presented the typical patterns of FC of the DMN (Figure 1). At rest, a decreased FC between the structures comprising the DMN was found in the WS group; specifically in one cluster comprising the precuneus, the calcarine and the posterior cingulate of the left hemisphere. The magnitude and graphic representation of these differences are presented in Table 1 and Figure 2, respectively. Moreover, a significant positive correlation was found between the FC of the right precuneus (peak MNI coordinates 6, −66, 52; cluster size 234 voxels; maximum *z*-score 3.30) and performance in the Block Design subtest in the clinical group (see Supplemental Figure 1).

Table 1 *Group Differences at Rest, in Brain Regions of the DMN Functional Maps (two-sample t-tests, corrected for multiple comparisons, p < 0.05).*

Condition	Regions	Peak MNI coordinates	Cluster size (voxels)	Maximum Z score
Control > WS	Posterior cingulate (left)	−6, −40, 22	424	3.48
	Precuneus (left)	−8, −60, 32		3.18
	Calcarine (left)	−4, −70, 16		3.18

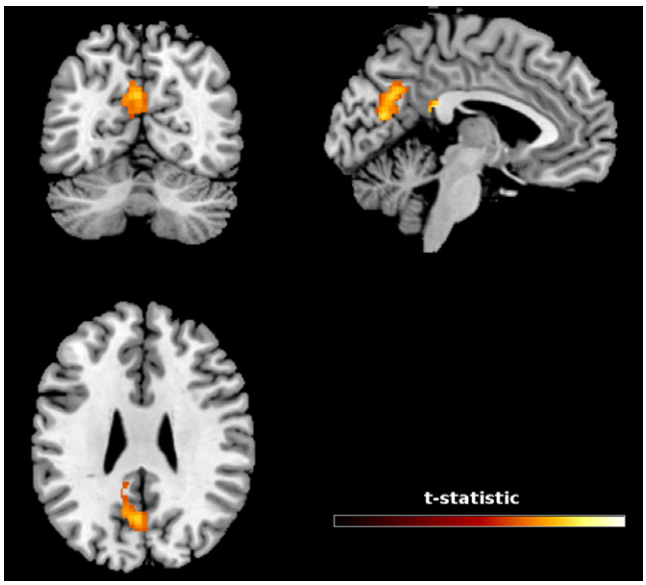

Figure 2 *Intra-resting state network group differences (WS and TD groups). Participants WS showed reduced FC within the DMN (defined by a 6 mm radius sphere centered on the PCC (1, −55, 17 MNI coordinates); statistical maps corrected for multiple comparisons (p < .05).*

Functional connectome approach

Testing the connectivity at the connectome level, a component of increased connectivity was found in the WS subjects at the threshold level of $p \leq .01$ (Figure 3), with a network significance of $p = .027$. The affected component extends from anterior to posterior areas in both hemispheres, and comprises 21 different nodes and 22 connections. The key regions in this connectome, identified as having three or more affected connections within the affected component, are the right frontal pole, the left paracentral lobule, the left inferior parietal, the right nucleus accumbens area and the right pallidum (please see Supplementary Table 1 for details). No other significant components were found. Moreover, regarding the distance between component nodes, both short-range and long-distance connectivity were equally affected, whereas 18 out of the 22 connections were inter-hemispheric. The connectome was visualized using BrainNet viewer (http://www.nitrc.org/projects/bnv/ (Xia, Wang & He, 2013).

Discussion

In this study we assessed the functional connectivity of the DMN in a group with WS and in a TD group. Moreover, we complemented this analysis with a functional connectome approach. While both groups presented the typical pattern of FC in the key regions of the DMN, a decreased DMN FC was observed in the WS group when compared with the typically developing group. These results are consistent with previous results showing a decreased connectivity within the DMN in participants with WS, when compared with TD and Down syndrome (Vega *et al.*, 2015). In addition, volumetric differences were not driving these DMN FC results, although a tendency for higher DMN volume in WS was observed, particularly in the area where a decreased FC was reported – the left posterior cingulate. This is a highly heterogeneous region, is part of the posterior hub of the DMN and displays an important role in cognition, specifically, in subserving memory, controlling the balance between internal and external thought, regulating the focus of attention (Leech & Sharp, 2014), and processing basic types of visual motion (Antal, Baudewig, Paulus & Dechent, 2008). Moreover, the posterior cingulate cortex is adjacent to the precuneus and is commonly referred to as the PCC/precuneus posterior hub of the DMN. The precuneus is also responsible for visuospatial imagery (Cavanna & Trimble, 2006) and together with the calcarine is also a region displaying a decreased FC in our WS group. Interestingly, we found that the right precuneus FC was positively associated with performance in a visuospatial task in WS (Block Design subtest). These posterior hub DMN regions are involved in visuospatial processes and are responsible for visual processing, including execution or preparation of spatially guided behaviors (Astafiev, Shulman, Stanley, Snyder, Van Essen *et al.*, 2003). Our results suggest that alterations in the FC of these brain regions may be part of the neurobiological basis underlying one of the most distinctive phenotypic features demonstrated by individuals with WS – their prominent visuospatial construction impairments (Atkinson, Braddick, Anker, Curran, Andrew *et al.*, 2003; Farran & Jarrold, 2003). In fact, morphological alterations in these regions (e.g. altered patterns of cortical folding) and histometric abnormalities (e.g. increased cell packing density) have also been described in WS (Gaser *et al.*,

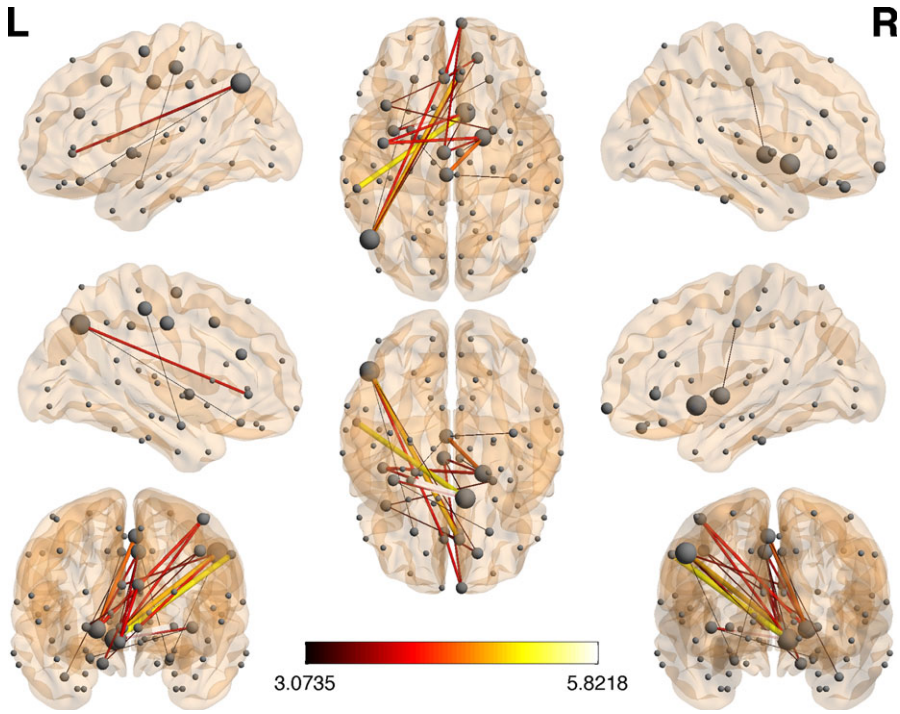

Figure 3 *Functional connectivity at the network level. WS participants displayed increased connectivity in a network comprising the right frontal pole, the left paracentral lobule, the left inferior parietal, the right nucleus accumbens area and the right pallidum as key regions.*

2006; Holinger, Bellugi, Mills, Korenberg, Reiss *et al.*, 2005) that are likely to be associated with the lack of volumetric regional differences described in these regions (Chiang, Reiss, Lee, Bellugi, Galaburda *et al.*, 2007).

At the whole brain connectome level, an increased FC component was found in the WS group compared to controls, with the right frontal pole, the left paracentral lobule, the left inferior parietal, the right nucleus accumbens area and the right pallidum brain regions being the key ROI regions. This result contrasts in direction with the ones found in the voxel-wise analysis, suggesting that further and more complex alterations might be at work. It seems to follow a similar tendency to the increased connectivity between networks observed in other neurodevelopmental disorders (Anderson, Nielsen, Ferguson, Burback, Cox *et al.*, 2013; Vega *et al.*, 2015) and is likely to reflect decreased ability to segregate information from large-scale association cortex into coherent networks (Anderson *et al.*, 2013; Fair, Dosenbach, Church, Cohen, Brahmbhatt *et al.*, 2007) and may be a more general feature of neurodevelopmental disorders (Vega *et al.*, 2015).

The FC patterns represent the spatial brain regions that are functionally synchronized over time, and therefore share statistical dependency/correlation (Friston, 2009). In children, these resting state networks are organized by anatomical proximity, as short-range connections present higher correlations than long-distance connectivity. This is a different pattern from what is observed in adults, suggesting a developmental trajectory of the brain FC (Goldenberga & Galvána, 2015). Indeed, intra-hemispheric FC between local nodes precedes the development of longer-distance inter-hemispheric connectivity (Fransson, Skiold, Horsch, Nordell, Blennow *et al.*, 2007; Goldenberga & Galvána, 2015; Lin, Zhu, Gao, Chen, Toh *et al.*, 2008). Our results showed increased inter-hemispheric FC characterized by a reduced lateralized distribution of the connectivity nodes, suggesting an immaturity of the brain FC patterns in WS. Moreover, these results are consistent with corpus callosum morphometric alterations, as well as high patterns of bilateral symmetry reported in WS (Sampaio *et al.*, 2013; Van Essen, Dierker, Snyder, Raichle, Reiss *et al.*, 2006). In fact, our results confirm the divergent patterns of FC in the DMN and other RSNs in several neurodevelopmental disorders (Anderson *et al.*, 2013; Kennedy & Courchesne, 2008a, 2008b; Menon *et al.*, 2004; Vega *et al.*, 2015).

Overall, we found that WS individuals present a reduced FC in the posterior hub of the DMN that was associated with a key feature of WS phenotype – visual-spatial cognition impairment. Importantly, these

functional alterations were not associated with structural/volumetric network changes. Our results also expand previous studies showing decreased FC in the DMN of individuals with WS (Vega *et al*., 2015) by reporting for the first time an increased global and interhemispheric FC in WS using a functional connectome approach.

Notwithstanding the promising evidence found in our study, our results should be interpreted with caution due to some limitations that should be addressed. First, there are some challenges to studying FC in neurodevelopmental disorders (Anderson *et al*., 2013) as it is prone to high levels of subject motion during scanning. While we tried to reduce the potential contamination of motion on FC with a motion scrubbing approach (Power *et al*., 2012), we had to exclude 30% of the sample due to motion artifacts. Therefore, the small sample size with a broad age range and a cross-sectional design preclude a complete and robust description of the WS FC patterns. Also, only the pattern of the DMN at rest was analyzed, not taking into account the importance of examining the dynamics of activation–deactivation of the DMN, during the transition from rest to task performance. With this study we have sought to enlighten the association between WS functional connectivity abnormalities and characteristic atypical social-cognitive aspects.

Acknowledgements

We are thankful to all study participants. This research was supported by FEDER funds through the Competitive Factors Operational Programme – COMPETE, by national funds from the Portuguese Foundation for Science and Technology (grant PTDC/PSI-PCL/115316/2009). This study was partially conducted at the Psychology Research Centre, University of Minho, and supported by the Portuguese Foundation for Science and Technology and the Portuguese Ministry of Education and Science through national funds and when applicable co-financed by FEDER under the PT2020 Partnership Agreement (UID/PSI/01662/2013).

References

Anderson, J.S., Nielsen, J.A., Ferguson, M.A., Burback, M.C., Cox, E.T., et al. (2013). Abnormal brain synchrony in Down Syndrome. *NeuroImage Clinical*, **2**, 703–715.

Antal, A., Baudewig, J., Paulus, W., & Dechent, P. (2008). The posterior cingulate cortex and planum temporale/parietal operculum are activated by coherent visual motion. *Visual Neuroscience*, **25** (1), 17–26.

Astafiev, S.V., Shulman, G.L., Stanley, C.M., Snyder, A.Z., Van Essen, D.C., et al. (2003). Functional organization of human intraparietal and frontal cortex for attending, looking, and pointing. *Journal of Neuroscience*, **23** (11), 4689–4699.

Atkinson, J., Braddick, O., Anker, S., Curran, W., Andrew, R., et al. (2003). Neurobiological models of visuospatial cognition in children with Williams syndrome: measures of dorsal-stream and frontal function. *Developmental Neuropsychology*, **23** (1–2), 139–172.

Behzadi, Y., Restom, K., Liau, J., & Liu, T.T. (2007). A component based noise correction method (CompCor) for BOLD and perfusion based fMRI. *NeuroImage*, **37** (1), 90–101.

Broyd, S.J., Demanuele, C., Debener, S., Helps, S.K., James, C.J., et al. (2009). Default-mode brain dysfunction in mental disorders: a systematic review. *Neuroscience and Biobehavioral Reviews*, **33** (3), 279–296.

Buckner, R.L., Andrews-Hanna, J.R., & Schacter, D.L. (2008). The brain's default network: anatomy, function, and relevance to disease. *Annals of the New York Academy of Sciences*, **1124**, 1–38.

Capitao, L., Sampaio, A., Fernandez, M., Sousa, N., Pinheiro, A., et al. (2011a). Williams syndrome hypersociability: a neuropsychological study of the amygdala and prefrontal cortex hypotheses. *Research in Developmental Disabilities*, **32** (3), 1169–1179.

Capitao, L., Sampaio, A., Sampaio, C., Vasconcelos, C., Fernandez, M., et al. (2011b). MRI amygdala volume in Williams Syndrome. *Research in Developmental Disabilities*, **32** (6), 2767–2772.

Cavanna, A.E., & Trimble, M.R. (2006). The precuneus: a review of its functional anatomy and behavioural correlates. *Brain*, **129** (Pt. 3), 564–583.

Chiang, M.C., Reiss, A.L., Lee, A.D., Bellugi, U., Galaburda, A.M., et al. (2007). 3D pattern of brain abnormalities in Williams syndrome visualized using tensor-based morphometry. *NeuroImage*, **36** (4), 1096–1109.

Desikan, R.S., Segonne, F., Fischl, B., Quinn, B.T., Dickerson, B.C., et al. (2006). An automated labeling system for subdividing the human cerebral cortex on MRI scans into gyral based regions of interest. *NeuroImage*, **31** (3), 968–980.

Dodd, H.F., Porter, M.A., Peters, G.L., & Rapee, R.M. (2010). Social approach in pre-school children with Williams syndrome: the role of the face. *Journal of Intellectual Disability Research*, **54** (3), 194–203.

Dykens, E.M., & Rosner, B.A. (1999). Refining behavioral phenotypes: personality-motivation in Williams and Prader-Willi syndromes. *American Journal of Mental Retardation*, **104** (2), 158–169.

Fair, D.A., Dosenbach, N.U., Church, J.A., Cohen, A.L., Brahmbhatt, S., et al. (2007). Development of distinct control networks through segregation and integration. *Proceedings of the National Academy of Sciences, USA*, **104** (33), 13507–13512.

Farran, E.K., & Jarrold, C. (2003). Visuospatial cognition in Williams syndrome: reviewing and accounting for the

strengths and weaknesses in performance. *Developmental Neuropsychology*, **23** (1–2), 173–200.
Fischl, B., Salat, D.H., Busa, E., Albert, M., Dieterich, M., et al. (2002). Whole brain segmentation: automated labeling of neuroanatomical structures in the human brain. *Neuron*, **33** (3), 341–355.
Fransson, P., Skiold, B., Horsch, S., Nordell, A., Blennow, M., et al. (2007). Resting-state networks in the infant brain. *Proceedings of the National Academy of Sciences, USA*, **104** (39), 15531–15536.
Friston, K. (2009). Causal modelling and brain connectivity in functional magnetic resonance imaging. *PLoS Biology*, **7** (2), e1000033.
Galaburda, A.M., & Bellugi, U. (2000). Multi-level analysis of cortical neuroanatomy in Williams syndrome. *Journal of Cognitive Neuroscience*, **12** (Suppl. 1), 74–88.
Gaser, C., Luders, E., Thompson, P.M., Lee, A.D., Dutton, R.A., et al. (2006). Increased local gyrification mapped in Williams syndrome. *NeuroImage*, **33** (1), 46–54.
Goldenberga, D., & Galvána, A. (2015). The use of functional and effective connectivity techniques to understand the developing brain. *Developmental Cognitive Neuroscience*, **12**, 155–164.
Gothelf, D., Searcy, Y.M., Reilly, J., Lai, P.T., Lanre-Amos, T., et al. (2008). Association between cerebral shape and social use of language in Williams syndrome. *American Journal of Medical Genetics, Part A*, **146A** (21), 2753–2761.
Greicius, M.D., Krasnow, B., Reiss, A.L., & Menon, V. (2003). Functional connectivity in the resting brain: a network analysis of the default mode hypothesis. *Proceedings of the National Academy of Sciences, USA*, **100** (1), 253–258.
Guerrero-Pedraza, A., McKenna, P.J., Gomar, J.J., Sarro, S., Salvador, R., et al. (2012). First-episode psychosis is characterized by failure of deactivation but not by hypo- or hyperfrontality. *Psychological Medicine*, **42** (1), 73–84.
Holinger, D.P., Bellugi, U., Mills, D.L., Korenberg, J.R., Reiss, A.L., et al. (2005). Relative sparing of primary auditory cortex in Williams syndrome. *Brain Research*, **1037** (1–2), 35–42.
Holt, D.J., Cassidy, B.S., Andrews-Hanna, J.R., Lee, S.M., Coombs, G., et al. (2011). An anterior-to-posterior shift in midline cortical activity in schizophrenia during self-reflection. *Biological Psychiatry*, **69** (5), 415–423.
Jones, W., Bellugi, U., Lai, Z., Chiles, M., Reilly, J., et al. (2000). Hypersociability in Williams syndrome. *Journal of Cognitive Neuroscience*, **12** (Suppl. 1), 30–46.
Jung, M., Kosaka, H., Saito, D.N., Ishitobi, M., Morita, T., et al. (2014). Default mode network in young male adults with autism spectrum disorder: relationship with autism spectrum traits. *Molecular Autism*, **5**, 35.
Kennedy, D.P., & Courchesne, E. (2008a). Functional abnormalities of the default network during self- and other-reflection in autism. *Social Cognitive and Affective Neuroscience*, **3** (2), 177–190.
Kennedy, D.P., & Courchesne, E. (2008b). The intrinsic functional organization of the brain is altered in autism. *NeuroImage*, **39** (4), 1877–1885.
Klein-Tasman, B.P., Li-Barber, K.T., & Magargee, E.T. (2011). Honing in on the social phenotype in Williams syndrome using multiple measures and multiple raters. *Journal of Autism and Developmental Disorders*, **41** (3), 341–351.
Korenberg, J.R., Chen, X.N., Hirota, H., Lai, Z., Bellugi, U., et al. (2000). Genome structure and cognitive map of Williams syndrome. *Journal of Cognitive Neuroscience*, **12** (Suppl. 1), 89–107.
Laing, E., Butterworth, G., Ansari, D., Gsödl, M., Longhi, E., et al. (2002). Atypical development of language and social communication in toddlers with Williams syndrome. *Developmental Science*, **5** (2), 233–246.
Leech, R., & Sharp, D.J. (2014). The role of the posterior cingulate cortex in cognition and disease. *Brain*, **137** (Pt. 1), 12–32.
Lin, W., Zhu, Q., Gao, W., Chen, Y., Toh, C.H., et al. (2008). Functional connectivity MR imaging reveals cortical functional connectivity in the developing brain. *American Journal of Neuroradiology*, **29** (10), 1883–1889.
Magalhaes, R., Marques, P., Soares, J., Alves, V., & Sousa, N. (2015). The impact of normalization and segmentation on resting-state brain networks. *Brain Connect*, **5** (3), 166–176.
Marenco, S., Siuta, M.A., Kippenhan, J.S., Grodofsky, S., Chang, W., et al. (2007). Genetic contributions to white matter architecture revealed by diffusion tensor imaging in Williams syndrome. *Proceedings of the National Academy of Sciences, USA*, **104** (38), 15117–15122.
Mars, R.B., Neubert, F.X., Noonan, M.P., Sallet, J., Toni, I., et al. (2012). On the relationship between the 'default mode network' and the 'social brain'. *Frontiers in Human Neuroscience*, **6**, 189.
Mason, M.F., Norton, M.I., Van Horn, J.D., Wegner, D.M., Grafton, S.T., et al. (2007). Wandering minds: the default network and stimulus-independent thought. *Science*, **315** (5810), 393–395.
Mayer, J.S., Roebroeck, A., Maurer, K., & Linden, D.E. (2010). Specialization in the default mode: task-induced brain deactivations dissociate between visual working memory and attention. *Human Brain Mapping*, **31** (1), 126–139.
Menon, V., Leroux, J., White, C.D., & Reiss, A.L. (2004). Frontostriatal deficits in fragile X syndrome: relation to FMR1 gene expression. *Proceedings of the National Academy of Sciences, USA*, **101** (10), 3615–3620.
Meyer-Lindenberg, A., Hariri, A.R., Munoz, K.E., Mervis, C.B., Mattay, V.S., et al. (2005). Neural correlates of genetically abnormal social cognition in Williams syndrome. *Nature Neuroscience*, **8** (8), 991–993.
Meyer-Lindenberg, A., Kohn, P., Mervis, C.B., Kippenhan, J.S., Olsen, R.K., et al. (2004). Neural basis of genetically determined visuospatial construction deficit in Williams syndrome. *Neuron*, **43** (5), 623–631.
Millman, K.J., & Brett, M. (2007). Analysis of functional magnetic resonance imaging in Python. *Computing in Science & Engineering*, **9** (3), 52–55.
Mitchell, J.P. (2008). Contributions of functional neuroimaging to the study of social cognition. *Current Directions in Psychological Science*, **17** (2), 142–146.

Munoz, K.E., Meyer-Lindenberg, A., Hariri, A.R., Mervis, C.B., Mattay, V.S., et al. (2010). Abnormalities in neural processing of emotional stimuli in Williams syndrome vary according to social vs. non-social content. *NeuroImage*, **50** (1), 340–346.

Pomarol-Clotet, E., Salvador, R., Sarro, S., Gomar, J., Vila, F., et al. (2008). Failure to deactivate in the prefrontal cortex in schizophrenia: dysfunction of the default mode network? *Psychological Medicine*, **38** (8), 1185–1193.

Power, J., Barnes, K.A., Snyder, A.Z., Schlaggar, B.L., & Peterson, S. (2012). Spurious but systematic correlations in functional connectivity MRI networks arise from subject motion. *NeuroImage*, **59** (3), 2142–2154.

Raichle, M.E., MacLeod, A.M., Snyder, A.Z., Powers, W.J., Gusnard, D.A., et al. (2001). A default mode of brain function. *Proceedings of the National Academy of Sciences, USA*, **98** (2), 676–682.

Reiss, A.L., Eckert, M.A., Rose, F.E., Karchemskiy, A., Kesler, S., et al. (2004). An experiment of nature: brain anatomy parallels cognition and behavior in Williams syndrome. *Journal of Neuroscience*, **24** (21), 5009–5015.

Reiss, A.L., Eliez, S., Schmitt, J.E., Straus, E., Lai, Z., et al. (2000). Neuroanatomy of Williams syndrome: a high-resolution MRI study. *Journal of Cognitive Neuroscience*, **12** (Suppl. 1), 65–73.

Sampaio, A., Bouix, S., Sousa, N., Vasconcelos, C., Fernandez, M., et al. (2013). Morphometry of corpus callosum in Williams syndrome: shape as an index of neural development. *Brain Structure and Function*, **218** (3), 711–720.

Sampaio, A., Fernandez, M., Henriques, M., Carracedo, A., Sousa, N., et al. (2009). Cognitive functioning in Williams syndrome: a study in Portuguese and Spanish patients. *European Journal of Paediatric Neurology*, **13** (4), 337–342.

Sampaio, A., Sousa, N., Fernandez, M., Henriques, M., & Goncalves, O.F. (2008). Memory abilities in Williams syndrome: dissociation or developmental delay hypothesis? *Brain and Cognition*, **66** (3), 290–297.

Singh, K.D., & Fawcett, I.P. (2008). Transient and linearly graded deactivation of the human default-mode network by a visual detection task. *NeuroImage*, **41** (1), 100–112.

Soares, J.M., Sampaio, A., Ferreira, L.M., Santos, N.C., Marques, F., et al. (2012). Stress-induced changes in human decision-making are reversible. *Translational Psychiatry*, **2**, e131.

Tzourio-Mazoyer, N., Landeau, B., Papathanassiou, D., Crivello, F., Etard, O., et al. (2002). Automated anatomical labeling of activations in SPM using a macroscopic anatomical parcellation of the MNI MRI single-subject brain. *NeuroImage*, **15** (1), 273–289.

Van der Fluit, F., Gaffrey, M.S., & Klein-Tasman, B.P. (2012). Social cognition in Williams syndrome: relations between performance on the social attribution task and cognitive and behavioral characteristics. *Frontiers in Psychology*, **3**, 197.

Van Essen, D.C., Dierker, D., Snyder, A.Z., Raichle, M.E., Reiss, A.L., et al. (2006). Symmetry of cortical folding abnormalities in Williams syndrome revealed by surface-based analyses. *Journal of Neuroscience*, **26** (20), 5470–5483.

Vega, J.N., Hohman, T.J., Pryweller, J.R., Dykens, E.M., & Thornton-Wells, T.A. (2015). Resting state functional connectivity in individuals with Down syndrome and Williams syndrome compared to typically developing controls. *Brain Connectivity*, **5** (8), 461–475.

von dem Hagen, E.A., Stoyanova, R.S., Baron-Cohen, S., & Calder, A.J. (2013). Reduced functional connectivity within and between 'social' resting state networks in autism spectrum conditions. *Social Cognitive and Affective Neuroscience*, **8** (6), 694–701.

Wechsler, D. (1991). *Wechsler Intelligence Scale for Children. Manual* (3rd edn.). San Antonio, TX: Psychological Corporation.

Wechsler, D. (1997). *Wechsler Adult Intelligence Scale. Manual* (3rd edn.). San Antonio, TX: Psychological Corporation.

Weng, S.J., Wiggins, J.L., Peltier, S.J., Carrasco, M., Risi, S., et al. (2010). Alterations of resting state functional connectivity in the default network in adolescents with autism spectrum disorders. *Brain Research*, **1313**, 202–214.

Woodward, N.D., Rogers, B., & Heckers, S. (2011). Functional resting-state networks are differentially affected in schizophrenia. *Schizophrenia Research*, **130** (1–3), 86–93.

Xia, M., Wang, J., & He, Y. (2013). BrainNet Viewer: a network visualization tool for human brain connectomics. *PLoS ONE*, **8** (7), e68910.

Zalesky, A., Fornito, A., & Bullmore, E.T. (2010). Network-based statistic: identifying differences in brain networks. *NeuroImage*, **53** (4), 1197–1207.

Received: 28 April 2015
Accepted: 24 March 2016

Supporting Information

Additional Supporting Information may be found online in the supporting information tab for this article:

Figure S1 Functional connectivity of the DMN and Block Design subtest in the WS group.

Table S1 Pair of Regions with Increased Connectivity in the WS Group at the Threshold Level.